Crystal structure and magnetic ordering of the rare-earth and Cu moments in $R Ba_2Cu_2NbO_8$ (R = Nd,Pr)

N. Rosov and J. W. Lynn
Reactor Radiation Division, National Institute of Standards and Technology, Gaithersburg, Maryland 20899
and Center for Superconductivity Research, Department of Physics, University of Maryland, College Park, Maryland 20742

H. B. Radousky and M. Bennahmias
University of California, Lawrence Livermore National Laboratory, Livermore, California 94550

T. J. Goodwin, P. Klavins, and R. N. Shelton
Department of Physics, University of California, Davis, California 95616
(Received 3 February 1993)

Using neutron diffraction, we have studied the crystal structure and magnetic ordering of the rare-earth and Cu moments in the layered perovskite systems $NdBa_2Cu_2NbO_8$ (Nd 2:2:1:8) and $PrBa_2Cu_2NbO_8$ (Pr 2:2:1:8). These are systems similar to $R Ba_2Cu_3O_{6+x}$ [R 1:2:3:(6+x)] for which the chain Cu-O layers have been fully replaced by layers of Nb-O octahedra. Powder profile refinements below 20 K show that both Nd 2:2:1:8 and Pr 2:2:1:8 are in space group $I4/mcm$, because the near-neighbor Nb-O octahedra are rotated about the c axis in opposite senses. The Cu moments are ordered below 375(10) K for Nd 2:2:1:8 and 340(15) K for Pr 2:2:1:8, with saturation moments in both cases of $0.5(1)\mu_B$. The near-neighbor Cu spins are aligned antiparallel, just as for the Cu "plane" ordering in R 1:2:3:(6+x). The rare-earth moments order at 1.69(5) and 12.6(1) K for Nd 2:2:1:8 and Pr 2:2:1:8, respectively, with saturated values of $\langle \mu_z \rangle = 0.74(5)\mu_B$ and $1.2(1)\mu_B$. The near-neighbor R spins, both in the ab plane and along the c axis, are also aligned antiparallel. As in the case of Pr 1:2:3:(6+x), the Pr sublattice of Pr 2:2:1:8 has an ordering temperature that is much higher than other rare-earth moments in these layered perovskites, suggesting that the Pr in Pr 2:2:1:8 experiences the same f-electron hybridization as has been observed in Pr 1:2:3:(6+x). The rare-earth ordering of both Nd 2:2:1:8 and Pr 2:2:1:8 is not completely three-dimensional in nature: rather, the ordering within the a-b plane is two-dimensional with only short-range order along the c axis. The presence of oxygen defects appears to affect the c-axis correlation length.

I. INTRODUCTION

The relationship between the superconductivity, the chain and plane copper magnetism, and the rare-earth magnetism in the $R Ba_2Cu_3O_{6+x}$ [R 1:2:3:(6+x)] compounds is of great interest, in part since there appears to be a significant coupling between the rare-earth ions and the state of the Cu-O planes. Initially,[1] evidence seemed to indicate that the rare-earth ions did not influence the superconducting behavior of the R 1:2:3:(6+x) compounds: With the exception of Pr,[2] all of the rare-earth ions that allow the formation of single-phase material also form superconducting materials with little change in critical temperature. Evidence for this decoupling was further strengthened by the fact that the R moments ordered antiferromagnetically (at low temperature) without significantly disrupting the superconductivity.[3] In addition, it appeared that the ordering of many of the large-moment rare-earth ions in R 1:2:3:7 occurred via dipolar interaction only: Er 1:2:3:7, Dy 1:2:3:7, $DyBa_2Cu_4O_8$ (Dy 2:4:8), and Gd 1:2:3:7 all order at temperatures that are consistent with a dipolar interaction, ranging from 0.6 to 2.2 K.

The most striking discrepancies from both of these observations occur for Pr 1:2:3:(6+x), Nd 1:2:3:(6+x), and Sm 1:2:3:(6+x).[4,5] The ordering temperature of the rare-earth moments due to dipolar interactions should be approximately two orders-of-magnitude less than those of the larger moment rare-earth ions; however, Pr 1:2:3:7 (Ref. 6) orders at 17 K and Nd 1:2:3:7 (Ref. 7) orders at 0.52 K. In addition, changing the oxygen content changes the rare-earth ordering temperature of Pr 1:2:3:(6+x) and Nd 1:2:3:(6+x). The ordering temperature of Pr 1:2:3:6 decreases by between 5 K (Ref. 8) and 10 K (Ref. 9). Even more dramatically, the long-range order in the Nd 1:2:3:(6+x) initially disappears[10,11] on decreasing x from 1, and then ultimately occurs at 1.5 K for $x \approx 0$, three times higher than the ordering temperature for $x \approx 1$. In addition, the x dependence of the orthorhombic-tetragonal transition in both the Nd and Pr compounds, and the lower superconducting plateau in Nd 1:2:3:(6+x), are significantly different from that of Y 1:2:3:(6+x).[12]

One approach to studying the coupling between R and the Cu-O subsystem is to determine the effect of substituting other (nonmagnetic) elements for some of the Cu. To this end, a new class of compounds, $R Ba_2Cu_2NbO_8$

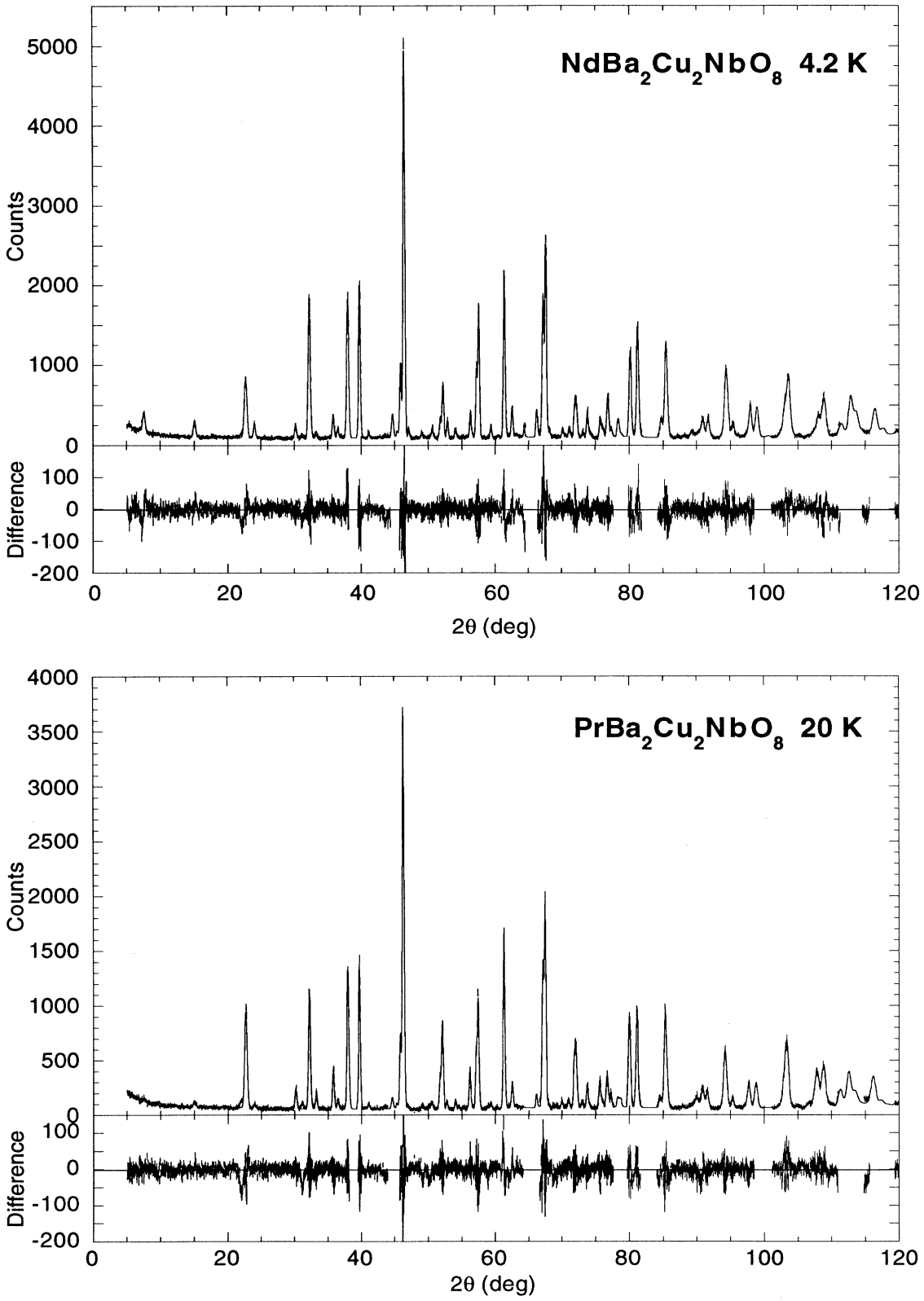

FIG. 1. High-resolution powder-diffraction pattern and Rietveld refinement fit of $NdBa_2Cu_2NbO_8$ (top) and $PrBa_2Cu_2NbO_8$ (bottom) at $T=5$ and 20 K, respectively, for $5° \leq 2\theta \leq 120°$ with $\lambda = 1.5454$ Å neutrons. Data have been excluded from the regions containing Bragg scattering from the Al sample can. The difference between the data and the refinement is shown below each diffraction pattern.

(R 2:2:1:8), has been prepared,[13,14] in which the Cu(1) chain layer of R 1:2:3:$(6+x)$ has been replaced by a layer of Nb-O octahedra. This has the effect of removing one of the magnetic components and the possibility of removing the intrinsic oxygen defects due to the coordination requirements of the Nb ions. Previous work on various R 2:2:1:8 compounds (R = Pr, La, and Nd) (Refs. 14–16) has shown them to be nonsuperconducting; in fact, they are excellent insulators. The rare-earth ion in Pr 2:2:1:8 has been observed, via susceptibility measurements, to order at 12 K, whereas no rare-earth ordering had been observed in Nd 2:2:1:8 down to 2 K.

We report here on neutron diffraction measurements made on Nd 2:2:1:8 and Pr 2:2:1:8. We have performed low-temperature high-resolution structural determinations using powder Rietveld refinement. In addition, we have observed the ordering of the plane Cu moments in both compounds at $\sim$350 K, established that the Pr moments order antiferromagnetically in Pr 2:2:1:8 at 12 K, and observed the antiferromagnetic ordering of the Nd moments in Nd 2:2:1:8 at 1.7 K.

II. SAMPLE CHARACTERIZATION AND CRYSTAL STRUCTURE

Powder samples of Nd 2:2:1:8 and Pr 2:2:1:8 were prepared by conventional solid-state reaction techniques, using stoichiometric amounts of 99.99% pure Pr_6O_{11}, $BaCO_3$, CuO, Nb_2O_5, and Nd_2O_3, as described elsewhere.[16] Previous x-ray-diffraction measurements have shown no observable impurity phases; however, the present neutron-diffraction data show several impurity peaks (e.g., at $2\theta \approx 22.04°$ and $2\theta \approx 30.98°$ for $\lambda = 1.5454$ Å) in both Nd 2:2:1:8 and Pr 2:2:1:8 that are less than 1% of the most intense sample reflections.

Diffraction patterns over a range of scattering angle $5° \leq 2\theta \leq 120°$ (see Fig. 1) of 10-g powder samples of Nd 2:2:1:8 and Pr 2:2:1:8 were taken with $\lambda = 1.5454$ Å neutrons on BT-1, the five-detector high-resolution powder diffractometer of the National Institute of Standards and Technology Research Reactor (NBSR). Angular collimations were 10′-20′-10′ full width at half maximum (FWHM), before and after the monochromator and after the sample, respectively. Both diffraction patterns were taken at low temperature, although well above the ordering temperature of the rare-earth ion. The Nd 2:2:1:8 measurement was made in a fixed temperature liquid ^{4}He cryostat at $T = 4.2$ K, and the Pr 2:2:1:8 measurement was made at $T = 20$ K in a closed-cycle He refrigerator. The refinements were carried out using the Rietveld method,[17] adapted to the multicounter diffractometer and modified to include the background parameters.[18]

Rietveld refinements of these patterns confirm that the structure is space group $I4/mcm$ as reported previously for La 2:2:1:8,[19] with lattice parameters, fractional positions, and anisotropic thermal factors as shown in Tables I and II. The χ values for the fits are close to unity, indicating that the overall fit to the data is very good. The largest deviations of the data from the fits (see Fig. 1) are less than three standard deviations. We initially freed the occupancies of all the elements, and determined that the occupancies of all atoms but the oxygen deviated from nominal stoichiometry by less than three standard devia-

TABLE I. Lattice parameters (a,b,c), fractional positions (x,y,z), occupancies (N), anisotropic thermal factors (B_{ij}), nuclear (R_N), unweighted (R_P), weighted (R_w) and expected (R_e) agreement factors, and the goodness-of-fit ($\chi = R_w/R_e$) for $PrBa_2Cu_2NbO_8$ at $T = 20$ K. The lineshapes are described by a Pearson VII function with $M = 9$. The refinement is to space group $I4/mcm$. Quantities enclosed in square brackets are fixed.

$PrBa_2Cu_2NbO_8$ $T = 20$ K
$a = b = 5.5782(1)$ Å, $c = 23.8893(7)$ Å
$R_N = 3.64$, $R_P = 6.99$, $R_w = 10.41$, $R_e = 7.51$, $\chi = 1.39$

Pr	$x = [\frac{1}{2}]$	$y = [0]$	$z = 0.2558(6)$	$N = [1]$
		$B = 0.5(2)$		
Ba	$x = [\frac{1}{2}]$	$y = [0]$	$x = 0.0974(1)$	$N = [2]$
	$B_{11} = B_{22} = 0.03(10)$		$B_{33} = 0.62(15)$	
	$B_{12} = -0.3(2)$		$B_{13} = B_{23} = [0]$	
Nb	$x = [0]$	$y = [0]$	$z = [0]$	$N = [1]$
	$B_{11} = B_{22} = 0.15(9)$	$B_{12} = B_{13} = B_{23} = [0]$	$B_{33} = 0.53(17)$	
Cu(2)	$x = [0]$	$y = [0]$	$z = 0.17834(10)$	$N = [2]$
	$B_{11} = B_{22} = 0.14(6)$	$B_{12} = B_{13} = B_{23} = [0]$	$B_{33} = 0.49(10)$	
O(1)	$x = [0]$	$y = [0]$	$z = 0.08143(15)$	$N = 2.00(2)$
	$B_{11} = B_{22} = 0.54(12)$	$B_{12} = B_{13} = B_{23} = [0]$	$B_{33} = 1.0(2)$	
O(2)	$x = -0.2510(3)$	$y = [x + \frac{1}{2}]$	$z = 0.18612(8)$	$N = 3.99(3)$
	$B_{11} = B_{22} = 0.28(7)$		$B_{33} = 0.84(12)$	
	$B_{12} = 0.13(9)$		$B_{13} = B_{23} = -0.12(6)$	
O(4)	$x = -0.2122(4)$	$y = [x + \frac{1}{2}]$	$z = [0]$	$N = 2.03(2)$
	$B_{11} = B_{22} = 0.94(11)$		$B_{33} = 1.4(2)$	
	$B_{12} = 0.48(16)$		$B_{13} = B_{23} = [0]$	

TABLE II. Lattice parameters (a,b,c), fractional positions (x,y,z), occupancies (N), anisotropic thermal factors (B_{ij}), nuclear (R_N), unweighted (R_P), weighted (R_w) and expected (R_e) agreement factors, and the goodness-of-fit ($\chi=R_w/R_e$) for $NdBa_2Cu_2NbO_8$ at $T=4.2$ K. The lineshapes are described by a Pearson VII function with $M=12$. The refinement is to space group $I4/mcm$. Quantities enclosed in square brackets are fixed.

$NdBa_2Cu_2NbO_8$, $T=4.2$ K
$a=b=5.5689(1)$ Å, $c=23.8820(6)$ Å
$R_N=3.80$, $R_P=5.78$, $R_w=8.24$, $R_e=6.31$, $\chi=1.31$

Nd	$x=[\frac{1}{2}]$	$y=[0]$	$z=[\frac{1}{4}]$	$N=[1]$
	$B_{11}=B_{22}=0.01(7)$	$B_{12}=B_{13}=B_{23}=[0]$	$B_{33}=0.38(12)$	
Ba	$x=[\frac{1}{2}]$	$y=[0]$	$z=0.09778(10)$	$N=[2]$
	$B_{11}=B_{22}=0.14(8)$		$B_{33}=0.43(11)$	
	$B_{12}=-0.07(14)$		$B_{13}=B_{23}=[0]$	
Nb	$x=[0]$	$y=[0]$	$z=[0]$	$N=[1]$
	$B_{11}=B_{22}=0.20(7)$	$B_{12}=B_{13}=B_{23}=[0]$	$B_{33}=0.87(13)$	
Cu(2)	$x=[0]$	$y=[0]$	$z=0.17894(7)$	$N=[2]$
	$B_{11}=B_{22}=0.26(4)$	$B_{12}=B_{13}=B_{23}=[0]$	$B_{33}=0.47(7)$	
O(1)	$x=[0]$	$y=[0]$	$z=0.08204(11)$	$N=1.96(2)$
	$B_{11}=B_{22}=0.39(9)$	$B_{12}=B_{13}=B_{23}=[0]$	$B_{33}=0.84(13)$	
O(2)	$x=-0.25153(24)$	$y=[x+\frac{1}{2}]$	$z=0.18687(6)$	$N=3.91(2)$
	$B_{11}=B_{22}=0.10(5)$		$B_{33}=1.05(9)$	
	$B_{12}=0.11(7)$		$B_{13}=B_{23}=-0.08(5)$	
O(4)	$x=-0.2093(3)$	$y=[x+\frac{1}{2}]$	$z=[0]$	$N=1.99(2)$
	$B_{11}=B_{22}=0.81(9)$		$B_{33}=0.42(14)$	
	$B_{12}=0.17(12)$		$B_{13}=B_{23}=[0]$	

tions. The final refinement was thus performed with only the oxygen occupancy free and all other occupancies fixed at nominal stoichiometry. The resulting occupancies indicate that the Nd compound is slightly oxygen deficient—$NdBa_2Cu_2NbO_{7.86(4)}$—and that the Pr compound is stoichiometric—$PrBa_2Cu_2NbO_{8.02(4)}$.

The anisotropic thermal factors of Nd and Pr in R 2:2:1:8 were initially found to be substantially different, with isotropic values ($B=[B_{11}+B_{22}+B_{33}]/3$) of 0.13 Å^2 for Nd and 1.02 Å^2 for Pr. The difference was particularly large along the c axis. As the freed Pr occupancy agreed with the nominal stoichiometry, the increased value of B for Pr could not be explained by a deficiency in the Pr occupancy. We therefore refined the structure while allowing the position of the Pr ion to be disordered along the c axis. The resulting structure had the Pr ion displaced by 0.139(2) Å from its initial special position of $\frac{1}{2},0,\frac{1}{4}$ to $\frac{1}{2},0,\frac{1}{4}\pm0.0058(6)$, while the isotropic thermal factor decreased by a factor of 2 to 0.5(2) Å^2.

The successful refinement to space group $I4/mcm$, rather than the simpler space group $P4/mmm$, results from the fact that Nb-O octahedra are alternately rotated around the c axis by $\sim6.5°$ (for Nd 2:2:1:8), with the sense of the rotation staggered while proceeding to nearest neighbors in the ab plane and along the c axis. This is classic soft-mode behavior typical of many perovskites, for example, La_2CuO_4.[20] The Cu(2)-O pyramids are also slightly rotated about the c axis, but by a much smaller amount, $\sim0.35°$ (for Nd 2:2:1:8). Again, near neighbors in the ab plane and along the c axis are rotated in the opposite sense. Proceeding along the c axis, the rotations of the adjoining Cu(2)-O pyramids and Nb-O octahedra occur in the opposite sense:

($z=0$)	($z\approx\frac{1}{6}$)	($z\approx\frac{1}{3}$)	($z=\frac{1}{2}$)	. . .
Nb-O	Cu-O	Cu-O	Nb-O	. . .
$+6.5°$	$-0.35°$	$+0.35°$	$-6.5°$	. . .

The bond lengths inferred from the refinement indicate that the only substantial difference between the Pr 2:2:1:8 and the Nd 2:2:1:8 structures is the R-O(2) distance, which is about 0.6% longer for the Pr-O(2) bond than for the Nd-O(2) bond (see Table III). This is reversed from the behavior observed in Pr 1:2:3:7 and Nd 1:2:3:7, where the Nd-O(2) bond is about 0.7% longer. The Nb-O distances are nearly unaffected by the rare-earth substitution, and are longer [~0.1 Å longer for Nb-O(1)] than the corresponding Cu(1)-O distances in R 1:2:3:7.

III. MAGNETIC NEUTRON DIFFRACTION

The magnetic ordering of both Nd 2:2:1:8 and Pr 2:2:1:8 was studied using BT-9 and BT-4, which are triple-axis spectrometers at NBSR, both of which we operated in two-axis mode for these measurements. Diffraction scans were made at $\lambda=2.35$ Å on BT-9 and $\lambda=2.444$ Å on BT-4, using a pyrolytic graphite monochromator and filter, and typical collimations of 40′ FWHM before the monochromator, between the monochromator and sample, and between the sample and detector.

A. Theoretical considerations

The magnetic scattering we observed exhibits both two-dimensional (2D) and three-dimensional (3D) behavior. The diffraction patterns expected as a result of

TABLE III. Bond lengths (Å) from structure determinations of Nd 2:2:1:8, Pr 2:2:1:8, La 2:2:1:8, Nd 1:2:3:7, Pr 1:2:3:7, and Dy 1:2:3:7. The *R* 2:2:1:8 determinations are all at low temperature (≤ 20 K) and the *R* 1:2:3:7 determinations are at room temperature.

	Nd 2:2:1:8[a]	Pr 2:2:1:8[a]	La 2:2:1:8[b]	Nd 1:2:3:7[c]	Pr 1:2:3:7[d]	Dy 1:2:3:7[e]
R-O(2)	2.4703(17)	2.4872(21)	2.534(2)	2.479(2)	2.462(3)	2.424(10)
	2.4895(18)	2.5003(22)	2.527(2)	2.454(2)	2.435(2)	2.369(11)
Ba-O(2)	2.8907(24)	2.8896(30)	2.883(3)	2.940(2)	2.981(3)	2.992(15)
	2.9071(22)	2.9009(29)	2.890(3)	2.943(2)	2.962(13)	2.974(15)
Ba-O(1)	2.8097(5)	2.8150(7)	2.823(0)	2.767(3)	2.769(1)	2.747(2)
Nb-O(1)[f]	1.9592(27)	1.9456(37)	1.946(2)	1.853(2)	1.849(3)	1.870(21)
Nb-O(4)[f]	1.9949(4)	1.9946(5)	1.996(3)	1.959(2)	1.964(1)	1.915(1)
Cu(2)-O(2)	1.9780(2)	1.9810(3)	1.987(2)	1.947(2)	1.950(1)	1.932(2)
Cu(2)-O(1)	2.3143(31)	2.3148(40)	2.283(3)	2.266(2)	2.254(4)	2.294(21)

[a]Present work.
[b]Reference 16.
[c]Reference 9.
[d]C. K. Lowe-Ma and T. A. Vanderah, Physica C **201**, 233 (1992).
[e]M. Machida, N. Achiwa, N. Koyano, I. Shibuya, M. Hikita, and A. Katsui, Jpn. J. Appl. Phys. **27**, L1866 (1988).
[f]These are the Cu(1)-O(1) and Cu(1)-O(4) distances for *R* 1:2:3:7.

this behavior have been extensively discussed by Zhang and co-workers,[21,22] and we will only briefly describe the patterns resulting from 2D and 3D ordering.

At sufficiently high temperatures, there are no magnetic correlations, and the magnetic scattering is spread uniformly though reciprocal space. As the system becomes ordered with decreasing temperature, most of this paramagnetic scattering becomes concentrated into coherent Bragg scattering at the reciprocal lattice vectors, τ. Since for 3D ordering the real-space lattice vectors define a 3D lattice, so do the possible τ and thus the scattering associated with long-range order occurs only at specific Bragg points. In the case of a powder sample, the Bragg points are averaged over a spherical shell of radius $|\tau|$ and the diffraction measurement observes each of these shells at a scattering angle 2θ defined by

$$\theta=\sin^{-1}\left[\frac{\lambda|\tau|}{4\pi}\right] . \tag{1}$$

In the usual case of diffraction from a collinear 3D magnetic structure, we can write the integrated intensity from a powder as[23]

$$I_M=C\left[\frac{\gamma e^2}{2mc^2}\right]^2\langle\mu_z\rangle^2 f^2(\tau) \times\langle 1-(\hat{\tau}\cdot\hat{\mathbf{M}})^2\rangle\frac{M_{hkl}\left|\sum_j e^{-W_j}e^{i\tau\cdot\mathbf{r}_j}\right|^2}{\sin\theta\sin 2\theta} . \tag{2}$$

C is the instrumental constant, the quantity in large brackets is the scattering length equivalent to $1\mu_B$, -0.27×10^{-12} cm, $\hat{\mathbf{M}}$ and $\hat{\tau}$ are unit vectors in the direction of the spin and τ, $\langle\mu_z\rangle$ is the thermal average of the ordered moment, $\langle 1-(\hat{\tau}\cdot\hat{\mathbf{M}})^2\rangle$ is averaged over all possible domains, and M_{hkl} is the multiplicity of the reflection. The summation is over all the sites at position $\mathbf{r}_j$ in the unit cell, where W_j is the Debye-Waller factor for the jth atom. Absorption effects can be safely neglected for the present materials.

The case of diffraction from a 2D lattice is essentially the same, save that the real-space lattice extends in only two dimensions. As a result, the momentum transfer is restricted in only two dimensions, and the Bragg peaks are extended along the third dimension into Bragg rods. Since the momentum transfer is only defined in two dimensions, there is a minimum transfer, but no maximum, that characterizes a particular reflection. As a result, the powder average peaks at some $|\mathbf{Q}_{\min}|$, and then decreases slowly, rather than exhibiting the sharp, symmetric, peaks that occur in the 3D case. The powder pattern thus has asymmetric peaks, where the degree of asymmetry depends inversely on the 2D correlation length. A powder average, over all possible orientations of reciprocal space, gives an intensity for the hk Bragg reflection of[24]

$$I_{hk}=C'\left[\frac{L}{\sqrt{\pi}\lambda}\right]^{1/2}\frac{M_{hk}|F_{hk}|^2\int_0^\infty e^{-(x^2-a)^2}dx}{(\sin\theta)^{3/2}} , \tag{3}$$

where L is a parameter that represents the size of a domain within the 2D layers, $a=(2L\sqrt{\pi}/\lambda)(\sin\theta-\sin\theta_B)$, and θ_B is the Bragg angle corresponding to $|\mathbf{Q}_{\min}|$.

If the system is ordered in two dimensions and has short-range order in the third dimension, we expect the Bragg rods to develop "corrugations" with increased intensity in the vicinity of the incipient 3D Bragg points and decreased intensity away from the Bragg points.[22] The powder pattern will then have peaks at the Bragg angles given by Eq. (1); however, these peaks will be asymmetric, though less so than the purely 2D patterns, and the peaks will be broader than those resulting from 3D long-range order. This is the case we observe in the present materials.

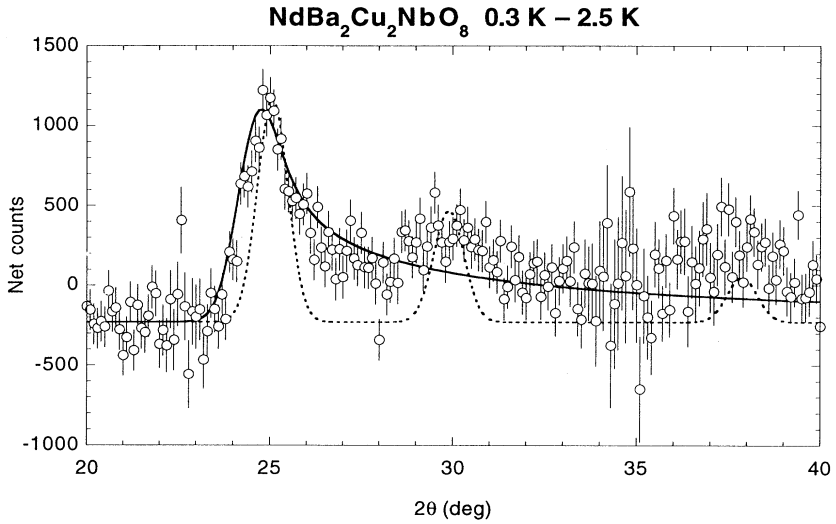

FIG. 2. Difference between diffraction patterns of $NdBa_2Cu_2NbO_8$ at $T=0.3$ and 2.5 K taken over the range $20° \leq 2\theta \leq 40°$ with $\lambda=2.35$ Å neutrons. The positions of the peaks indicate that the nearest-neighbor Nd spins are antiferromagnetically staggered both in and out of the *ab* plane, while the relative intensities indicate that the Nd moment is directed along the *c* axis. The asymmetric broadening of the magnetic peaks indicates that the magnetic order is long range in the *ab* plane, but only short range along the *c* axis. For comparison, the solid curve indicates the diffraction pattern expected for purely 2D order for Eq. (3) and the dotted curve indicates the diffraction pattern expected for purely 3D order.

B. Rare-earth magnetism

The magnetic ordering of the rare-earth ions in *R* 1:2:3:$(6+x)$ displays a great deal of variety. Superconducting Nd 1:2:3:6.9 undergoes 3D antiferromagnetic ordering at $T_N \approx 0.54$ K with the Nd moments alternating along all three axes.[7,25] As a result, magnetic $m/2\,n/2\,l/2$ Bragg peaks (m, n, and l odd) are observed. For lower oxygen concentrations, the long-range 3D order is suppressed, and only short-range 2D correlations are observed below $T \sim 1.5$ K.[10] The short-range 3D correlations, which are clearly visible in the diffraction pattern below T_N, are enhanced with further decrease of the oxygen concentration, until $x \leq 0.3$, whereupon long-range 3D order (below $T_N \approx 1.5$ K) is restored. A similar propensity to frustration along the *c* axis, due to structural intergrowths, is observed in the coupled bilayer system $Dy_2Ba_4Cu_7O_{15}$ (Dy 2:4:7).[22] In this case, the ordering is only two-dimensional and the coupling between members of a bilayer is predominantly ferromagnetic; however, a significant number of antiferromagnetically coupled layers also exist.

We made measurements on Nd 2:2:1:8, over the range $0.3 \leq T \leq 375$ K, in a pumped ^{3}He cryostat below 10 K and a closed-cycle He refrigerator above 10 K. The Pr 2:2:1:8 sample was measured over the range $4.2 \leq T \leq 350$ K, in a flow-type ^{4}He cryostat. For both samples we performed scans over a range in scattering angle of $5° \leq 2\theta \leq 65°$ at both the lowest temperature possible (0.3 K for Nd 2:2:1:8 and 4.2 K for Pr 2:2:1:8) and a temperature above the rare-earth ordering temperature (2.5 K for Nd 2:2:1:8 and 20 K for Pr 2:2:1:8). The difference between the high- and low-temperature scans, assuming no structural distortion, gives the magnetic diffraction pattern (see Figs. 2 and 3), if the sample has ordered between these two temperatures. For both Nd 2:2:1:8 and Pr 2:2:1:8, the positions of the peaks at $2\theta=25°$, 29.9°, and 37.9° can be indexed as the 101, 103,

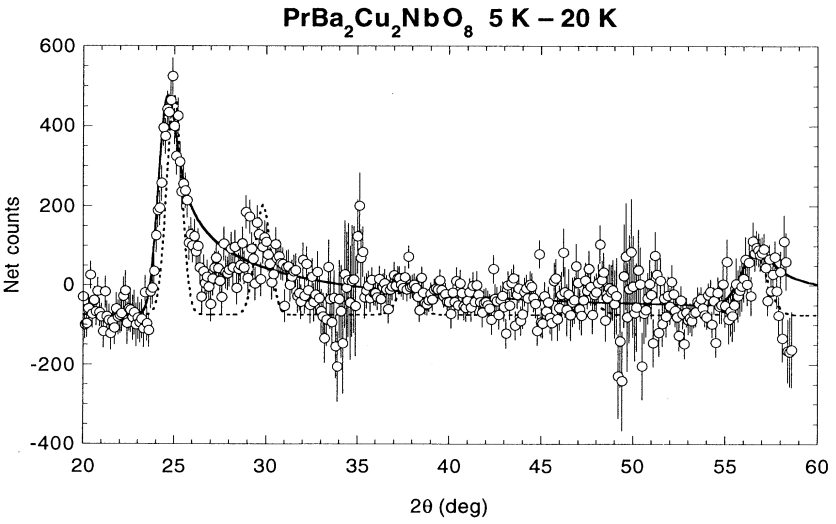

FIG. 3. Difference between diffraction patterns of $PrBa_2Cu_2NbO_8$ at $T=4.2$ and 20 K taken over the range $20° \leq 2\theta \leq 58.6°$ with $\lambda=2.35$ Å neutrons. The positions of the peaks indicate that the nearest-neighbor Pr spins are antiferromagnetically staggered both in and out of the *ab* plane, while the relative intensities indicate that the Nd moment is directed along the *c* axis. The asymmetric broadening of the magnetic peaks indicates that the magnetic order is long range in the *ab* plane, but only short range along the *c* axis. For comparison, the solid curve indicates the diffraction pattern expected for purely 2D order from Eq. (3) and the dotted curve indicates the diffraction pattern expected for purely 3D order. Note the presence of the 21 reflection at ~57°, in addition to the 10 reflection at ~25°.

and 105 reflections for the R 2:2:1:8 nuclear unit cell. These, respectively, correspond to the $\frac{1}{2}\frac{1}{2}\frac{1}{2}$, $\frac{1}{2}\frac{1}{2}\frac{3}{2}$, and $\frac{1}{2}\frac{1}{2}\frac{5}{2}$ reflections of the equivalent R 1:2:3:$(6+x)$ nuclear unit cell. As a result, we can say that the nearest-neighbor Nd and Pr moments are aligned antiparallel both in the ab plane and along the c axis, which is the same structure observed in the rare-earth ordering for Nd 1:2:3:$(6+x)$ (Ref. 7) and Pr 1:2:3:7 (Ref. 6). The relative intensities of the peaks are consistent with the Nd and Pr moments directed along the c axis, which is the same direction as the rare earth moments in the corresponding R 1:2:3:7 compounds. The saturation value of the Nd moment of $0.74(5)\mu_B$ is consistent with that observed in Nd 1:2:3:7,[7] whereas the saturation value of $1.2(1)\mu_B$ for the Pr moment is significantly higher than the $0.7\mu_B$ measured for Pr 1:2:3:7.[6]

We have also measured the peak intensity at $2\theta=25°$ as a function of T to determine the temperature dependence of the square of the order parameter, as shown in Figs. 4 and 5. The ordering temperature of the Nd moment, as determined by a least-squares fit to a mean-field model, is $T_N=1.69(5)$ K, which is appreciably higher than the ordering temperature of 0.5 K observed for Nd 1:2:3:7,[7] but is similar to $T_N=1.5$ K for Nd 1:2:3:6. The Pr moment orders, by a similar determination, at 12.6(1) K, which is somewhat lower than $T_N=17$ K measured for Pr 1:2:3:7,[6] but is close to that of Pr 1:2:3:6.[8,9]

The magnetic diffraction peaks resulting from the rare-earth ordering are seen to be strongly asymmetric, and while they do appear at 3D Bragg reflection positions (as the dotted curves show), clearly reveal that we do not have conventional 3D long-range order. On the other hand, the solid curves in Figs. 2 and 3 are diffraction curves according to the purely 2D theory [Eq. (3)], and indicate that we cannot neglect correlations along the c axis. The diffraction pattern that we observed is thus indicative of a combination of 2D and 3D behavior. We see both the highly asymmetric diffraction peak that one would expect from a 2D powder pattern and broadened peaks at the positions expected from a 3D powder pattern. The 2D component of the powder pattern for Nd 2:2:1:8 is essentially at our resolution limit, which implies an in-plane correlation length on the order of 200 Å or more. The widths of the 3D peaks imply a c-axis correlation length of 25(10) Å. Thus, the rare-earth order of Nd 2:2:1:8 is long range in the ab plane, whereas correlations along the c axis only extend across approximately two rare-earth planes. The Pr in-plane correlation is also long range. We estimate the correlation length along the c axis to be 7(1) Å, slightly less than the separation between the rare-earth planes and less than half of the Nd 2:2:1:8 c-axis correlation length.

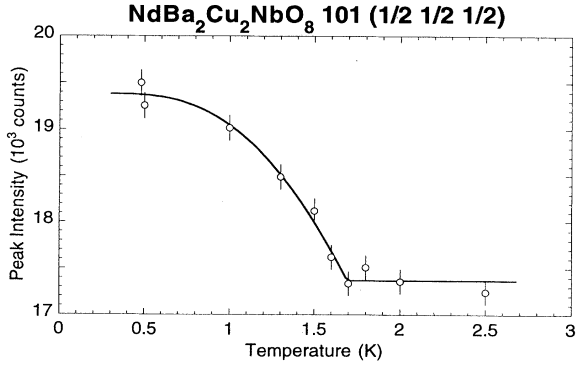

FIG. 4. Peak intensity of the scattering at $2\theta=24.94°$ (the position of the 101 reflection) vs T for $NdBa_2Cu_2NbO_8$. The solid curve is a fit of the square of a mean-field order parameter to the data. The fitted ordering temperature for the Nd moments is $T_N=1.69(5)$ K.

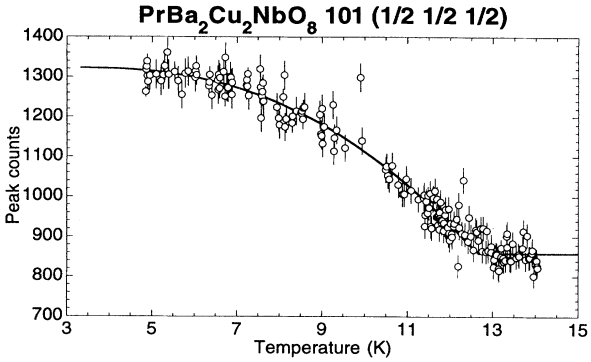

FIG. 5. Peak intensity of the scattering at $2\theta=24.87°$ (the maximum of the 101 reflection) vs T for $PrBa_2Cu_2NbO_8$. The solid curve is a fit of the square of a mean-field order parameter to the data. The fitted ordering temperature for the Pr moments is $T_N=12.65(7)$ K.

C. Cu magnetic order

In the original R $Ba_2Cu_3O_{6+x}$ [R 1:2:3:$(6+x)$] compounds, there are three Cu layers per unit cell.[26] Two of these are the so-called "plane" layers that contain Cu(2) ions, which are surrounded by oxygen in a pyramidal coordination. The remaining "chain" layer contains Cu(1) ions, which are in a square planar coordination. The two types of layers exhibit different magnetic behavior, which changes as a function of oxygen concentration.[27,28] At $x\approx 0$, in those compounds that display superconductivity at $x\approx 1$, the Cu(2) spins order at $T_{Np}\approx 525$ K. This plane ordering has a simple antiferromagnetic structure, with nearest-neighbor Cu(2) spins antiparallel in all three directions. Since there are two Cu(2) layers per unit cell, and only one Cu(2) per unit cell in the a and b directions, the plane ordering is characterized by magnetic $m/2\,n/2\,l$ Bragg reflections, where l is an integer. At lower temperatures, the chain spins have been observed to order, but in the R 2:2:1:8 materials the Cu chain spins have been replaced by nonmagnetic Nb, and we do not expect this complication. As a result, we anticipated that the magnetic ordering of the Cu(2) layers would be manifested solely as the plane ordering of the R 1:2:3:$(6+x)$ compounds, with magnetic $m/2\,n/2\,l$ Bragg reflections [$(m+n)/2\,(m-n)/2\,2l$ reflections in the R 2:2:1:8 nuclear unit cell]. We therefore concentrat-

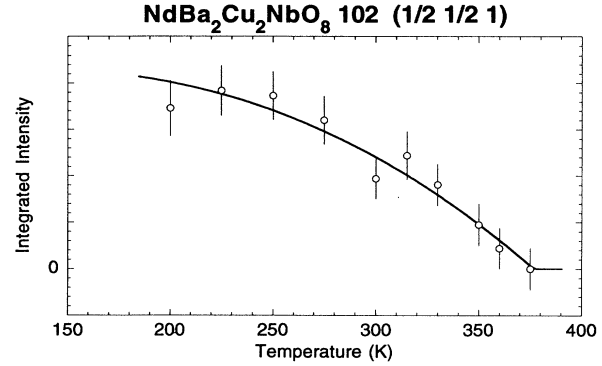

FIG. 6. Integrated intensity of the 102 reflection of $NdBa_2Cu_2NbO_8$ vs T. The solid curve is a fit of the square of a mean-field order parameter to the data. The fitted ordering temperature for the Cu moments is $T_N=375(10)$ K.

ed on a small peak observed at $2\theta=26.9°$, which corresponds to the expected position at the $\frac{1}{2}\frac{1}{2}2$ reflection (the 102 reflection in the R 2:2:1:8 nuclear unit cell). We measured the integrated intensity of the 102 reflection in the temperature ranges 200 K $\leq T \leq$ 375 K for Nd 2:2:1:8 and 50 K $\leq T \leq$ 350 K for Pr 2:2:1:8 (see Figs. 6 and 7). The intensities of the 102 peak for both Pr 2:2:1:8 and Nd 2:2:1:8 go to zero at about 350 K. A fit of the 102 integrated intensities to a mean-field model gives $T_N=340(15)$ K for Pr 2:2:1:8 and $T_N=375(10)$ K for Nd 2:2:1:8. These ordering temperatures are consistent with the observed plane ordering temperature $T_{Np}=370$ K (Ref. 29) of Pr 1:2:3:$(6+x)$ (for $0.2 \leq x \leq 0.65$), which is not superconducting for any x. Using Eq. (2), and comparing the intensity of a structural peak with the 102 intensity, we find that the saturation Cu moment for both Pr 2:2:1:8 and Nd 2:2:1:8 is $0.5(1)\mu_B$. We did not observe any half-integral reflections above the rare-earth ordering temperature, nor did we expect to, as there are no magnetic chain layer sites that can order.

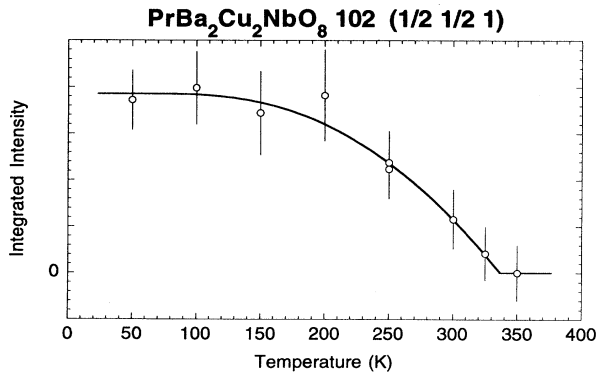

FIG. 7. Integrated intensity of the 102 reflection of $PrBa_2Cu_2NbO_8$ vs T. The solid curve is a fit of the square of a mean-field order parameter to the data. The fitted ordering temperature for the Cu moments is $T_N=340(15)$ K.

IV. DISCUSSION AND CONCLUSIONS

We have studied the crystal structure, the antiferromagnetic ordering of the Cu spins, and the rare-earth magnetic order of the nonsuperconducting layered perovskites $NdBa_2Cu_2NbO_{7.86(4)}$ and $PrBa_2Cu_2NbO_{8.02(4)}$ by neutron diffraction. Powder Rietveld refinements at low temperature (below 20 K) indicate that both Nd 2:2:1:8 and Pr 2:2:1:8 are in space group $I4/mcm$, with the Nb-O octahedra and the Cu(2)-O pyramids rotated about the c axis. The Pr ionic volume is approximately 2% larger than that of Nd. In addition, the Pr position was disordered, with the Pr shifted 0.137 Å away from the $\frac{1}{2},0,\frac{1}{4}$ position along the c axis. The Nd compound was slightly oxygen deficient and the Pr compound was stoichiometric within fitting error.

The ordering of the Cu(2) moments is similar to the plane ordering observed in the R 1:2:3:$(6+x)$ compounds.[16] There is no Cu(1) chain layer to complicate the copper magnetism, since the Cu(1) have been replaced by nonmagnetic Nb in R 2:2:1:8. The Cu(2) moments in Nd 2:2:1:8 and Pr 2:2:1:8 order at $T_N=340(15)$ and 370(10) K, respectively, ordering temperatures that are similar to the Cu plane ordering temperature observed in Pr 1:2:3:$(6+x)$. The saturation Cu(2) moments are the same in both Nd 2:2:1:8 and Pr 2:2:1:8, $\langle \mu_z \rangle = 0.5(1)\mu_B$, which is less than the $0.8\mu_B$ observed for the plane Cu moments in Nd 1:2:3:$(6+x)$ (Ref. 27) and Pr 1:2:3:$(6+x)$ (Ref. 29).

The rare-earth ordering occurs at 12.7(1) and 1.69(5) K for Pr 2:2:1:8 and Nd 2:2:1:8, respectively. The magnetic powder-diffraction patterns for both compounds indicate that the nearest neighbors in the ab plane and along the c axis are antiferromagnetically aligned. The Pr and Nd saturation moments are 1.2(1) and $0.74(5)\mu_B$, respectively, and the data are consistent with the moments pointing along the c axis. Both compounds exhibit short range order along the c axis, while within the ab plane the ordering is essentially long range in nature. The correlations along the c axis extend for about two rare-earth layers for Nd 2:2:1:8; however, the correlations extend for less than one interlayer distance in Pr 2:2:1:8. We remark that until recently, all systems that displayed 2D behavior also displayed parasitic 3D ordering.[30] Now, however, Nd 1:2:3:6.45 (Ref. 10), Pr 2:2:1:8, Nd 2:2:1:8, and Dy 2:4:7 (Ref. 22) have all been shown to display 2D order in the ab plane and correlations along the c axis, and Dy 2:4:8 (Ref. 21) displays only 2D long-range order down to the lowest temperatures observed, $T \approx 50$ mK.

We note that the subtle differences between the low-temperature c-axis correlation lengths for Pr 2:2:1:8 and Nd 2:2:1:8 may be related to the oxygen defects. The crystallographic refinement for Nd 2:2:1:8 indicates that it is significantly defective in oxygen content, with about 2% of the oxygens missing, mainly in the O(2) site in the Cu(2) plane. These O(2) oxygen sites are the nearest-neighbors to the rare-earth ion, and as a result, the crystal-field environment of some of the rare-earth ions will be disrupted[31] by the presence of oxygen defects, possibly causing the misalignment of the rare-earth spin from the c axis. On the other hand, for Pr 2:2:1:8 the ox-

ygen sites are fully populated, within error, and the c-axis correlation length is much less, $\xi=7(1)$ Å, than the 25(10) Å correlation length of Nd 2:2:1:8. In the undefected R 2:2:1:8 structure, there is no net coupling between the rare-earth planes, as there is no net moment in the antiferromagnetically ordered planes. We speculate, therefore, that the misalignment of the rare-earth moments, due to the presence of oxygen defects, may increase the coupling between the rare-earth planes by removing the condition of no net moment on an antiferromagnetically ordered rare-earth plane. The observation that Pr 2:2:1:8 has a shorter interplane correlation length than Nd 2:2:1:8, despite having a larger saturation moment and a higher ordering temperature, and thus larger coupling between planes, can therefore be explained by noting that the present sample of Pr 2:2:1:8 was determined to have no oxygen defects. The rare-earth order may therefore depend sensitively on the oxygen defect content, as has been previously observed for Nd 1:2:3:$(6+x)$.[10]

ACKNOWLEDGMENTS

Work at Maryland is supported by the National Science Foundation, Grant No. DMR 89-21878. Research at UC Davis is supported by the NSF, Grant No. DMR 90-21029 and the Air Force, Grant No. F49620-92-J-0514. Research at LLNL is supported by DOE Contract No. W-7405-ENG-48.

[1]P. H. Hor, R. L. Meng, Y. Q. Wang, L. Gao, Z. J. Huang, J. Bechtold, K. Forster, and C. W. Chu, Phys. Rev. Lett. **58**, 1891 (1987).

[2]L. Soderholm, K. Zhang, D. G. Hinks, M. A. Beno, J. E. Jorgensen, C. U. Segre, and I. K. Schuller, Nature (London) **328**, 604 (1987).

[3]A review of the rare-earth ordering is given by J. W. Lynn, in *High-Temperature Superconductivity,* edited by J. W. Lynn (Springer-Verlag, Berlin, 1990) p. 268.

[4]B. W. Lee, J. M. Ferreira, Y. Dalichaouch, M. S. Torikachvili, K. N. Yang, and M. B. Maple, Phys. Rev. B **37**, 2368 (1988).

[5]A. P. Ramirez, L. F. Schneemeyer, and J. V. Waszczak, Phys. Rev. B **36**, 7145 (1987).

[6]W.-H. Li, J. W. Lynn, S. Skanthakumar, T. W. Clinton, A. Kebede, C.-S. Jee, J. E. Crow, and T. Mihalisin, Phys. Rev. B **40**, 5300 (1989).

[7]K. N. Yang, J. M. Ferreira, B. W. Lee, M. B. Maple, W.-H. Li, J. W. Lynn, and R. W. Erwin, Phys. Rev. B **40**, 10 963 (1989).

[8]M. E. López-Morales, D. Ríos-Jara, J. Tagüeña, R. Escudero, S. La Placa, A. Bezinge, V. Y. Lee, E. M. Engler, and P. M. Grant, Phys. Rev. B **41**, 6655 (1990).

[9]G. Wortmann and I. Felner, Solid State Commun. **75**, 981 (1990).

[10]T. W. Clinton, J. W. Lynn, B. W. Lee, M. Buchgeister, and M. B. Maple, J. Appl. Phys. **73**, 6320 (1993).

[11]P. Allenspach, M. B. Maple, S. I. Yoo, and M. J. Kramer, J. Appl. Phys. **73**, 6317 (1993).

[12]H. Shaked, B. W. Veal, J. Faber, Jr., R. L. Hitterman, U. Balachandran, G. Tomlins, H. Shi, L. Morss, and A. P. Paulikas, Phys. Rev. B **41**, 4173 (1990).

[13]A. Ichinose, T. Wada, H. Yamauci, and S. Tanaka, J. Ceramic Soc. Jpn., Int. Ed. **97**, 1053 (1989).

[14]N. Murayama, E. Sudo, K. Kani, A. Tsuzuki, S. Kawakami, M. Awano, and Y. Torii, Jpn. J. Appl. Phys. **27**, L1623 (1988).

[15]H. B. Radousky, J. C. O'Brien, M. J. Bennahmias, P. Klavins, C. A. Smith, J. M. Link, T. J. Goodwin, and R. N. Shelton, in *Layered Superconductors: Fabrication, Properties, and Applications,* edited by D. T. Shaw *et al.*, MRS Symposia Proceedings No. 275 (Materials Research Society, Pittsburgh, 1992), p. 113.

[16]M. Bennahmias, J. C. O'Brien, H. B. Radousky, T. J. Goodwin, P. Klavins, J. M. Link, C. A. Smith, and R. N. Shelton, Phys. Rev. B **46**, 11 986 (1992).

[17]H. M. Rietveld, J. Appl. Crystallogr. **2**, 65 (1969).

[18]E. Prince, in National Bureau Standards Technical Note 1117, edited by F. J. Shorten, 1980, p. 8.

[19]M.-J. Rey, P. Dehaudt, J. Joubert, and A. W. Hewat, Physica C **167**, 162 (1990).

[20]R. J. Birgeneau, C. Y. Chen, D. R. Gabbe, H. P. Henssen, M. A. Kastner, C. H. Peters, P. J. Picone, T. Thio, T. R. Thurston, H. L. Tuller, J. D. Axe, P. Boni, and G. Shirane, Phys. Rev. Lett. **59**, 1329 (1987).

[21]H. Zhang, J. W. Lynn, W.-H. Li, T. W. Clinton, and D. E. Morris, Phys. Rev. B **41**, 11 229 (1990).

[22]H. Zhang, J. W. Lynn, and D. E. Morris, Phys. Rev. B **45**, 10 022 (1992).

[23]G. E. Bacon, *Neutron Diffraction* (Clarendon, Oxford, 1975).

[24]B. E. Warren, Phys. Rev. **59**, 693 (1941).

[25]P. Fischer, B. Schmid, P. Brüesh, F. Stucki, and P. Unternährer, Z. Phys. B **74**, 183 (1989).

[26]A. Santoro, in *High-Temperature Superconductivity,* edited by J. W. Lynn (Springer-Verlag, Berlin, 1990), p. 84.

[27]W. Li, J. W. Lynn, and Z. Fisk, Phys. Rev. B **41**, 4098 (1990).

[28]H. Kadowaki, M. Nishi, Y. Yamada, H. Takeya, H. Takei, S. Shapiro, and G. Shirane, Phys. Rev. B **37**, 7932 (1988).

[29]N. Rosov, J. W. Lynn, G. Cao, J. W. O'Reilly, P. Pernambuco-Wise, and J. E. Crow, Physica C **204**, 171 (1992).

[30]J. W. Lynn, J. Alloys Compounds **181**, 419 (1992).

[31]J. Mesot, P. Allenspach, U. Staub, A. Furrer, H. Mutka, R. Osborn, and S. Bennington, Physica B **180-181**, 405 (1992).